Steel and Composite Structures, *Vol. 19*, *No. 6* (*2015*) *1501-1510*
DOI: http://dx.doi.org/10.12989/scs.2015.19.6.1501

Change of transmission characteristics of FSSs in hybrid composites due to residual stresses

In-Han Hwang [1], Heoung-Jae Chun [*1], Ik-Pyo Hong [2a], Yong-Bae Park [3b] and Yoon-Jae Kim [4c]

[1] *Mechanical Engineering*, *Yonsei University*, *Seodaemun*, *Seoul 120-749*, *Korea*
[2] *Electric wave Engineering*, *Kongju University*, *Seobook*, *Kongju 1223-24*, *Korea*
[3] *Electronic Engineering*, *Ajou University*, *Youngdong*, *Suwon 443-749*, *Korea*
[4] *Agency for Defence Development*, *Yuseong*, *Daejeon 305-152*, *Korea*

(*Received February 28*, *2013*, *Revised April 29*, *2014*, *Accepted July 10*, *2015*)

Abstract. The frequency selective surface (FSS) embedded hybrid composite materials have been developed to provide excellent mechanical and specific electromagnetic properties. Radar absorbing structures (RASs) are an example material that provides both radar absorbing properties and structural characteristics. The absorbing efficiency of an RAS can be improved using selected materials having special absorptive properties and structural characteristics and can be in the form of multi-layers or have a certain stacking sequence. However, residual stresses occur in FSS embedded composite structures after co-curing due to a mismatch between the coefficients of thermal expansion of the FSS and the composite material. In this study, to develop an RAS, the thermal residual stresses of FSS embedded composite structures were analyzed using finite element analysis, considering the effect of stacking sequence of composite laminates with square loop (SL) and double square loop (DSL) FSS patterns. The FSS radar absorbing efficiency was measured in the K-band frequency range of 21.6 GHz. Residual stress leads to a change in the deformation of the FSS pattern. Using these results, the effect of transmission characteristics with respect to the deformation on FSS pattern was analyzed using an FSS Simulator.

Keywords: fiber-reinforced composite materials; radar absorbing structure; thermal residual stress; FSS-embedded composite structures; square loop; double square loop

1. Introduction

Fiber-reinforced composite materials have outstanding mechanical and electrical properties such that they have been applied in commercial products as well as military components. Using the unique characteristics of composite materials, researchers have studied radar absorbing techniques, so called ‘Stealth’ technology. Stealth technology is very important in modern warfare because these materials can prevent aircraft from being detected by enemy radar and other tracking

*Corresponding author, Professor, E-mail: hjchun@yonsei.ac.kr
[a] Professor, E-mail: iphong@kongju.ac.kr
[b] Professor, E-mail: yong@ajou.ac.kr
[c] Researcher at ADD, E-mail: 78strephon@add.re.kr

Copyright © 2015 Techno-Press, Ltd.
http://www.techno-press.org/?journal=scs&subpage=8 ISSN: 1229-9367 (Print), 1598-6233 (Online)

systems. In order to maximize the performance of stealth techniques, the radar cross section (RCS) of weapon systems should be minimized because the distance detected by radar is inversely proportional to the fourth root of the RCS (Jenn 1995). There are two methods to reduce the RCS of weapon systems. One is to absorb electromagnetic waves incident to the fuselage of weapon systems via radar absorbing materials (RAMs) and radar absorbing structures (RASs), and the other is to either transmit some of the waves through the radome or to selectively reflect the remaining waves at the radome surface. A hybrid radome is a type of composite RAS usually consisting of composite material and an FSS. FSSs are composed of a periodic array consisting of conducting patches or aperture elements. FSSs are used as polarizers, space filters, and subreflectors in dual frequency antennas and as parts of radomes to control RCS by selectively absorbing or transmitting the incident electromagnetic wave according to frequency. Hybrid radomes not only selectively absorb the incident electromagnetic wave, but also provide structural stability.

Many numerical studies have been conducted to analyze electromagnetic wave characteristics and reflection characteristics of FSSs (Bradshaw 1989, Mittra *et al*. 1998, Vinoy 1996). Monacelli *et al*. (2005) designed and fabricated infrared frequency selective surfaces using periodic method of moments (PMM) software based on circuit-analog resonance of square loop conducting elements. Kim *et al*. (Kim *et al*. 2006) measured EM transmission characteristics of an RAS composed of E-glass/epoxy and single dipole FSS elements in the X-band frequency range using the free space method to determine the effects of the size of the dipole element and its periodicity in the array. Also, the structure stability of hybrid radome was investigated by developing a method for designing and fabricating hybrid structures. The radar absorbing capability of composite materials is obtained from materials that provide special absorptive properties (Chung 2001, Pinho *et al*. 2002) or structural characteristics such as a particular stacking sequence of composites (Matous and Dvorak 2003, Tretyakov and Maslovski 2003).

By nature, fiber-reinforced composites made of thermoset resins undergo a curing process during solidification. During the cure process, expansion or shrinkage caused by thermal mismatch and chemical reaction occurs, such that it is difficult to control the dimensions of the final part. Although a number of researchers have studied the residual stress and warpage of thermoset composites as functions of manufacturing conditions (Gigliotti *et al*. 2003, 2004) and thermal properties (Ito *et al*. 2000, Ressettos and Shen 1995), few researchers have studied residual stress of hybrid composites composed of heterogeneous materials. In addition, residual stresses in FSS-embedded composite structures have not been widely investigated. In this study, the thermal residual stresses of low-observable radomes incorporating stealth technology in the bonding layer of the co-cure bonded FSS-embedded composite structures were analyzed using finite element analysis, considering the effect of stacking sequence. Then, the effect of transmission characteristics, which were varied due to the change in deformation due to residual stresses, on FSS pattern were analyzed using Ansoft HFSS Ver 12.0.

2. Materials and method

2.1 Frequency selective surface and hybrid radome model

There are various element types of FSSs including the Jerusalem cross (JC), square loop (SL), hexagon element (HE), and ring (R), as shown in Fig. 1. (Munk 2000) Among these element types, the resonant frequency of the SL is reasonably stable with respect to changes in the incident angle

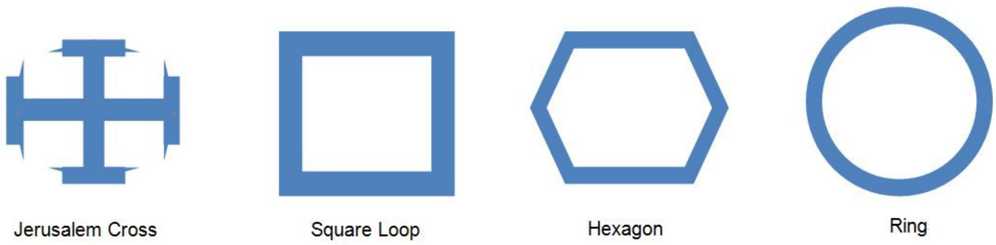

Fig. 1 Typical element types of FSSs

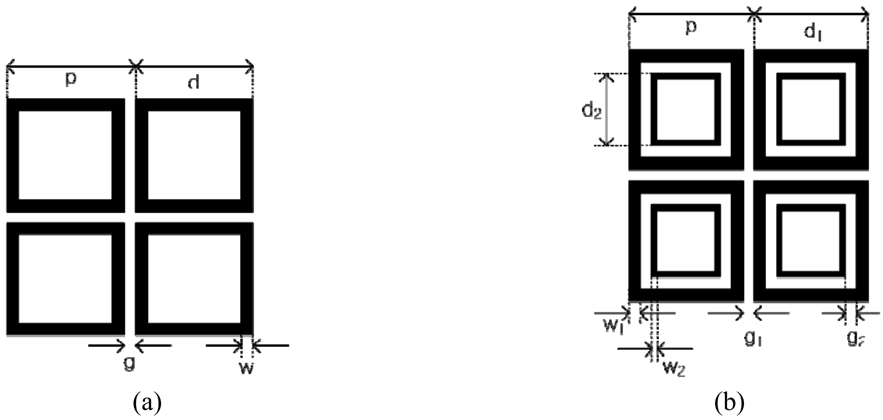

Fig. 2 Design parameters of FSSs: (a) Square loop; (b) Double square loop

and polarizations due to symmetrical shape. Therefore, an SL, as shown in Fig. 2(a), was designated as the basic pattern in this study. In additions, a double square loop (DSL) FSS was selected to compare the change of structural and electromagnetic characteristics. Particle swarm optimization (PSO) was applied for acquiring the optimized geometrical parameters of FSS patterns with a resonant frequency of 21.6 GHz (K-band) in our previous study. (Munk 2000) These predetermined dimensions of FSS patterns were used in this analysis and are shown in Tables 1 and 2.

Since the FSSs are in the form of periodic arrays, the unit cells enclosed by dotted lines are selected as representative elements, as shown in Fig. 3. A FSS is fabricated from a flexible copper-clad laminate composed of copper foil (thickness: 20 μm) and polyimide film (thickness: 40 μm), as shown in Fig. 4. As such, the overall representative volume model for studying the effects of the residual stresses in the FSS-embedded composite radome in this study is composed

Table 1 Design parameters of square loop

Parameters	Initial value (mm)
Gap of FSS (g)	0.6
Width of FSS (w)	0.26
Pitch of FSS (p)	4.44

Table 2 Design parameters of double square loop

Parameters	Initial value (mm)
Major gap of FSS (g_1)	1.46
Minor gap of FSS (g_2)	0.22
First width of FSS (w_1)	0.75
Second width of FSS (w_2)	0.36
Pitch of FSS (p)	7.79

of E-glass/epoxy composite laminates, copper foil, polyimide film and epoxy. The epoxy resin is considered as an adhesion material which fills the gap between the E-glass/epoxy composite laminate and the polyimide film. E-glass/epoxy composite laminates act as the load-bearing structure of the radome because of their high strength. The copper foil has excellent conductivity, and the polyimide film has low dielectric loss.

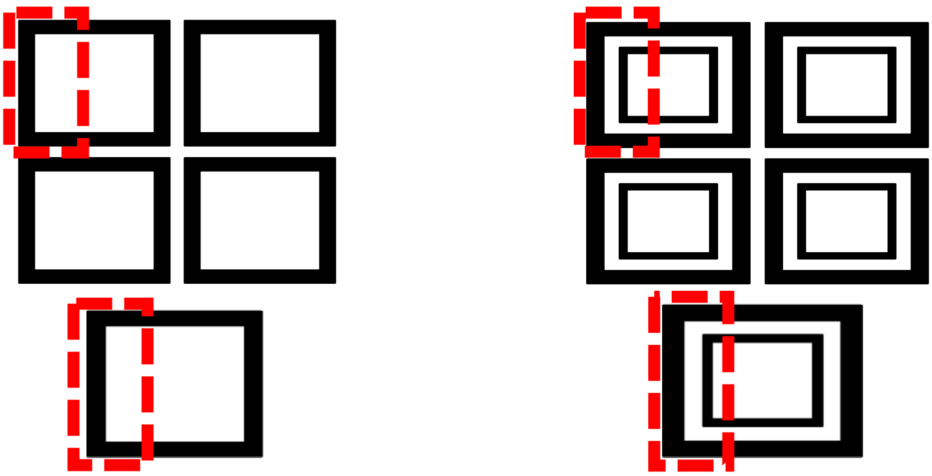

(a) (b)

Fig. 3 FSSs and unit cells: (a) Square loop; (b) Double square loop

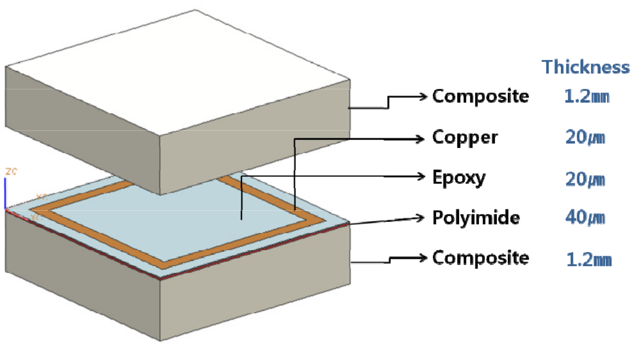

Fig. 4 Overall model of hybrid structure

Table 3 Material properties of E-glass/epoxy

Property	Symbol	Value
Longitudinal modulus	E_1	38.6 GPa
Transverse modulus	$E_2 = E_3$	8.27 GPa
In-plane shear modulus	G_{12}	2.3 GPa
Poisson's ratio	v_{12}	0.26
Longitudinal coefficient of thermal expansion	α_1	6.3 (10-6/°C)
Transverse coefficient of thermal expansion	α_2	20 (10-6/°C)
Transverse tensile strength	F_{3t}	65 MPa
Out-of-plane shear strength	F_{13}	40 MPa

Table 4 Material properties of copper, polyimide and epoxy

Property	Copper	Polyimide	Epoxy
Elastic modulus	110 GPa	2.5 GPa	4.3 GPa
Poisson's ratio	0.343	0.35	0.35
Coefficient of thermal expansion	16.4 (10-6/°C)	4.014 (10-6/°C)	45 (10-6/°C)

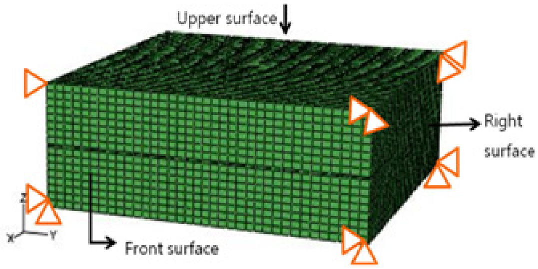

Fig. 5 Boundary and loading conditions

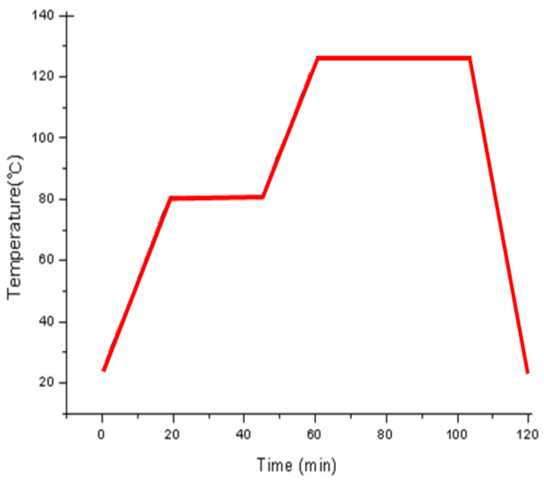

Fig. 6 Cure cycle used to co-cure E-glass/epoxy composite and FSS

2.2 Finite element modeling

The residual stresses in the hybrid structure were predicted by Abaqus 6.10, based on this three-dimensional finite element model which consists of eight node-coupled temperature and displacement elements of type C3D8T. The material properties of E-glass/epoxy composite, epoxy resin, copper and polyimide are shown in Tables 3 and 4. Eight plies of composite laminate skins were considered in the analysis. The stacking sequences of composite laminates were $[0]_8$, $[0/90]_4$, $[\pm 45]_4$, and $[0/\pm 45/90]_2$. Boundary and loading conditions of the FE-model are shown in Fig. 5. Symmetric boundary conditions were applied at the front, rear, right and left surfaces along the *y*-

Table 5 Maximum stresses and strains of copper FSS layer

	Square loop			Double square loop		
	Residual stress (MPa)	Strain of *x*-axes (10^{-3})	Strain of *y*-axes (10^{-3})	Residual stress (MPa)	Strain of *x*-axes (10^{-3})	Strain of *y*-axes (10^{-3})
$[0]_8$	31.2	-1.60	-2.00	37.6	-1.61	-2.04
$[0/90]_4$	19.0	-1.75	-1.67	20.7	-1.76	-1.71
$[\pm 45]_4$	17.8	-1.72	-1.72	20.5	-1.75	-1.75
$[0/\pm 45/90]_2$	19.8	-1.60	-1.72	20.9	-1.72	-1.75

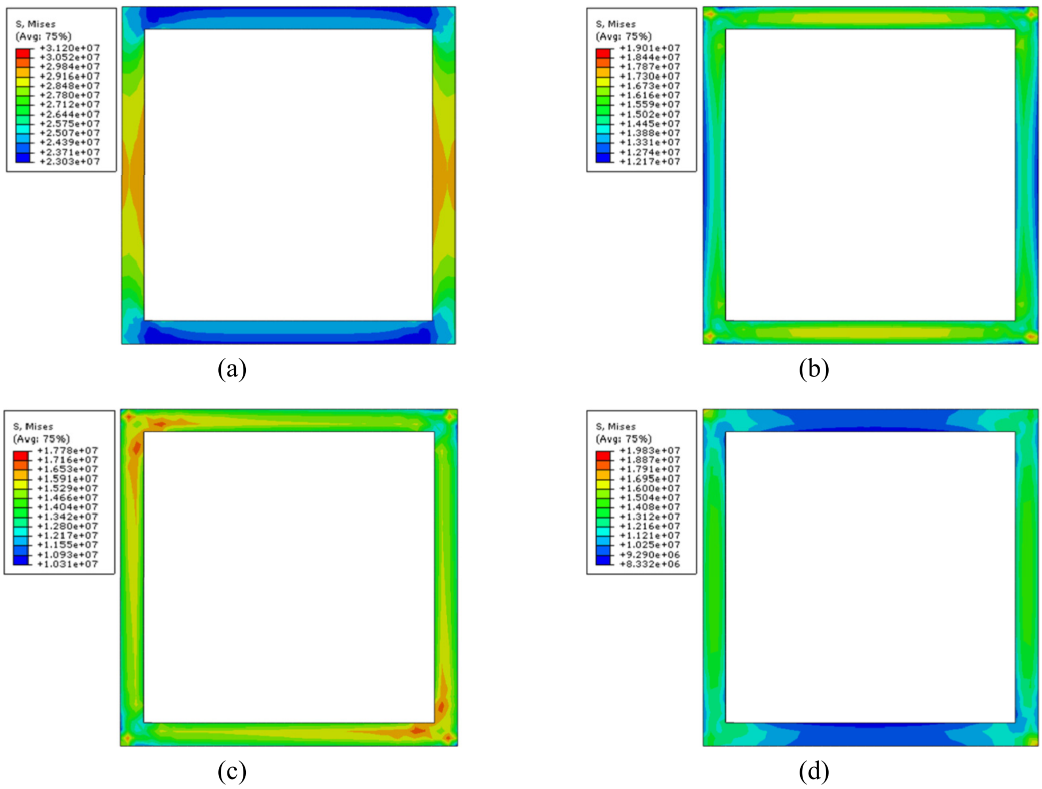

Fig. 7 Effective residual stress distributions of copper SL FSS: (a) $[0]_8$, (b) $[0/90]_4$, (c) $[\pm 45]_4$, (d) $[0/\pm 45/90]_2$

and *x*-axes. The lower surfaces were fixed in the *z*-direction. The thermal loading condition in finite element analysis was induced by cooling the hybrid structure from 125°C to 20°C, simulating the final cooling stage of co-cure bonding because it was assumed that the thermal residual stresses in the hybrid composites were developed after cross-linking of matrix and before the cooling stage. A typical curing procedure of the composite is shown in Fig. 6.

3. Results

The residual stresses led to a change in deformation of the FSS pattern in the hybrid composites with a resonant frequency of 21.6 GHz. Table 5 shows the maximum residual stress and strain values in copper FSS adjacent to composite layers in the hybrid composite laminates. The highest maximum residual stress and strain were produced in the $[0]_8$ stacking sequence. Residual stress distributions in the SL and DSL copper FSS patterns with different composite stacking sequences are shown in Figs. 7 and 8.

In terms of stacking sequence, the maximum strain was less in cross and angle ply relative to the uni-directional, which showed the maximum difference in thermal expansion. Moreover, the least residual stress and strain occurred in the $[\pm 45]_4$ stacking sequence.

Fig. 9 shows the results of the resonance frequency in the deformed metallic pattern due to

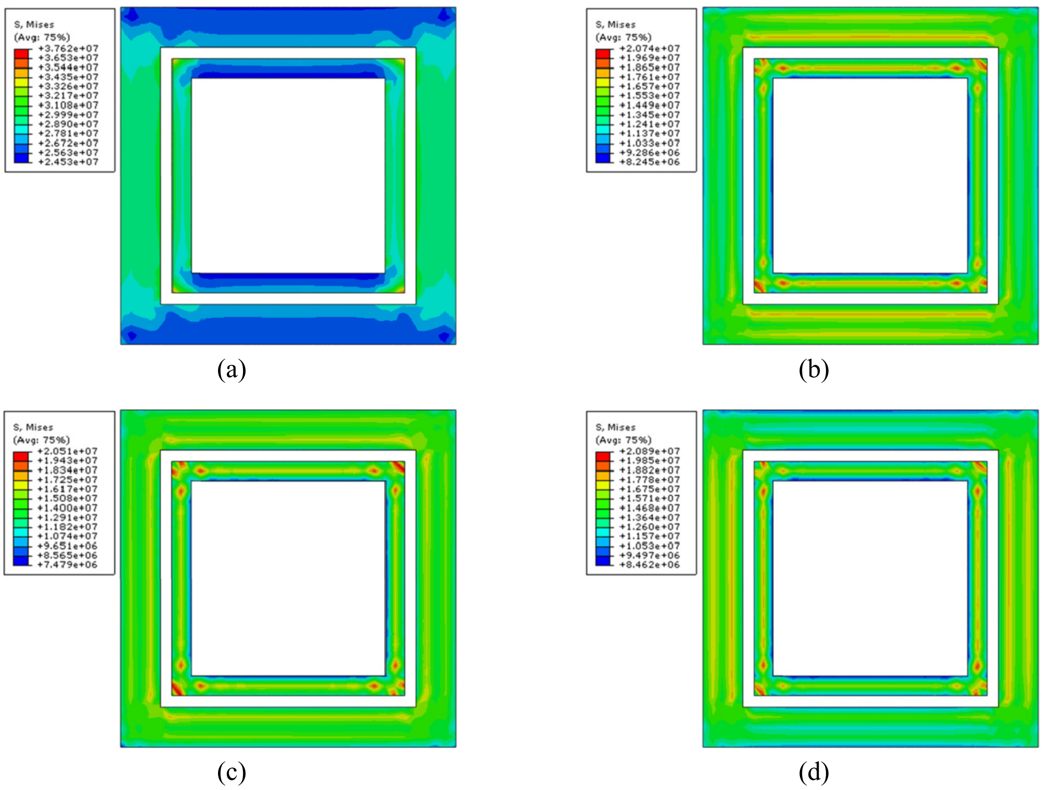

Fig. 8 Effective residual stress distributions of copper DSL FSS
(a) $[0]_8$; (b) $[0/90]_4$; (c) $[\pm 45]_4$; (d) $[0/\pm 45/90]_2$

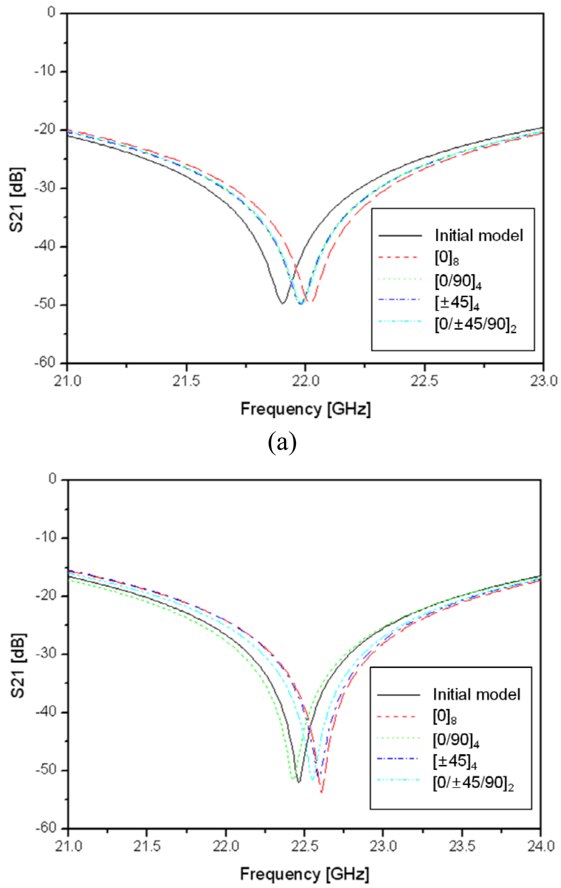

(a)

(b)

Fig. 9 Simulation results of resonant frequency in FSS: (a) Square loop; (b) Double square loop

Table 6 Ratios of resonant frequency shift compared with non deformed FSSs

Shift ratio of resonant frequency	$[0]_8$	$[0/90]_4$	$[\pm 45]_4$	$[0/\pm 45/90]_2$
Square loop	0.55%	0.37%	0.37%	0.37%
Double square loop	0.67%	0.13%	0.57%	0.4%

residual stresses. The initial SL FSS has resonant frequency of 21.9 GHz. The deformed model in $[0]_8$ stacking sequence shows 22.02 GHz as the resonant frequency, but the other deformed models shows same resonant frequency which is 21.98GHz. The DSL FSS prior to deformation has reflection characteristics of 22.46 GHz, and the those of deformed FSSs were 22.46 GHz, 22.43 GHz, 22.59 GHz and 22.55 GHz for stacking sequences of $[0]_8$, $[0/90]_4$, $[\pm 45]_4$, $[0/\pm 45/90]_2$, respectively.

Table 6 shows the shift ratio in transmission characteristics of FSSs before and after deformation. In comparison, the maximum shift ratio was obtained for stacking sequences of $[0]_8$, while those with $[\pm 45]_4$, $[0]_8$ and $[0/\pm 45/90]_2$ showed the minimum resonance frequency shift ratio.

4. Conclusions

In this study, stealth technology was integrated in composite structures with glass fiber-reinforced polymeric composite materials. Finite element analysis was applied to analyze thermal residual stresses of the FSS-embedded hybrid structures, considering the effect of stacking sequence. Then the effects of transmission characteristics, which varied due to the change in deformations caused by residual stresses, on FSS pattern were analyzed using Ansoft HFSS Ver 12.0.

The geometries of the conductor and the permittivity and dimensions of the dielectric substance as well as the stacking sequences of composite laminated skins in the FSS-embedded hybrid structures, which may change the characteristics of radio waves as well as states of residual stresses in embedded FSSs, are considered in FSS design in general. The results showed that the reflection characteristics were easily shifted depending on the stacking sequences in composites such that the bandwidth may be enlarged or reduced. However, at high frequency, it was likely that the resonance frequency would be shifted, and the band stop would likely be diminished. Also the residual stresses in embedded FSSs are strongly influenced by the stacking sequences in composites skins. Therefore, according to the above results, stacking sequence could also be one of the influential design parameters in FSS. These results are useful for designing highly integrated FSS-embedded composite structures.

Acknowledgments

This work has been supported by the Low Observable Technology Research Center Program of the Defense Acquisition Program Administration and the Agency for Defense Development of Republic of Korea.

References

Bradshaw, P. (1989), "Signature management and structural materials, Material and processing - move to the 90's", *Proceedings of Society for the Advancement of Material & Process Engineering*, Birmingham, UK, July.

Chung, D. (2001), "Electromagnetic interference shielding effectiveness of carbon materials", *Carbon*, **39**(2), 279-285.

Gigliotti, M., Wisnom, M. and Potter, K. (2003), "Development of curvature during the cure of AS4/8552 [0/90] unsymmetric composite plates", *Compos. Sci. Technol.*, **63**(2), 187-197.

Gigliotti, M., Jacquemin, F. and Vautrin, A. (2004), "On the maximum curvatures of 0/90 plates under thermal stress", *Compos. Struct.*, **68**(2), 177-184.

Ito, T., Suganuma, T. and Wakashima, K. (2000), "A micromechanics based analysis for tailoring glass fiber reinforced thermoplastic laminates with near zero coefficients of thermal expansion", *Compos. Sci. Technol.*, **60**(9), 1851-1861.

Jenn, D. (1995), *Radar and Laser Cross Section Engineering*, American Institute Aeronautics and Astronautics Inc., Washington, D.C., USA.

Jung, K., Chu, S. and Ahn, H. (2009), "Measurement and compensation of spring-back of a hybrid composite beam", *J.Compos. Mater.*, **41**(7), 851-864.

Kaini, I., Weily. R. and Esselle, P. (2006), "A novel absorb/transmit FSS for secure indoor wireless networks with reduced multipath fading", *IEEE microw*, *wirel. co*.,. **16**(6), 378-380.

Kim, C. and Lee, G. (2009), "Improvement of bonding characteristics between the frequency selective surface and E-glass/epoxy composites for stealth radomes", *J. Adhes. Sci. Technol.*, **23**(2), 215-227.

Kim, C., Chin, W., Lee, D. and Seo, I. (2006), "EM characteristics of the RAS composed of E-glass/epoxy composite and single dipole FSS element", *Compos. Struct.*, **75**(1-4), 601-609.

Kim, C., Lee, G., Seo, S. and Kim, H. (2008), "Low-observable radomes composed of composite sandwich constructions and frequency selective surfaces", *Compos. Sci. Technol.*, **68**(9), 2163-2170.

Lee, Y., Jeong, R., Hong, P., Lee, G., Chun, J. and Yook, G. (2011), "Simple design method of FSS radome analysis using equivalent circuit model", *IEICE. Electron. Expr.*, **8**(23), 2002-2009.

Liu, T., Cheng, F., Chu, Y. and Zhang, Y. (2007), "Absorbing properties of frequency selective surface absorbers with cross-shaped resistive patches", *Mate. Design.*, **28**(7), 2166-2171.

Matous, K. and Dvorak, G. (2003), "Optimization of electromagnetic absorption in laminated composite plates", *Trans. Magn.*, **39**(3), 1827-1835.

Mittra, R., Chan, C. and Cwik, T. (1998), "Techniques for analyzing frequency selective surfaces - a review", *Proceedings of the IEEE 1988*, Dec, **76**(12), 1593-1615.

Monacelli, B., Pryor, J., Munk, B., Kotter, D. and Boreman, G. (2005), "Infrared Frequency Selective Surface based on circuit-analog square loop design", *IEEE T Antenn. Propag.*, **53**(2), 745-752.

Munk, B. (2000), *Frequency Selective Surfaces*, Wiley, New York, NY, USA.

Pinho, M., Gregori, M., Nunes, R. and Soares, B. (2002), "Performance of radar absorbing materials by waveguide measurements for X and Kuband frequencies", *Eur. Polym. J.*, **38**(11), 2321-2327.

Ressettos, J. and Shen, X. (1995), "On the axial and interfacial shear stresses due to thermal mismatch in hybrid composite sheets", *Compos. Sci. Technol.*, **54**(4), 417-422.

Tretyakov, S. and Maslovski, S. (2003), "Thin absorbing structure for all incidence angles based on the use of a high-impedance surface", *Microw. Opt. Technol. Lett*,. **38**(3), 175-178.

Vinoy, K. (1996), *Radar Absorbing Materials from Theory to Design and Characterization*, (1st Ed.), Kluwer Academic Publisher, Boston, MA, USA.

CC